

# NUMERICAL ASSESSMENT OF LONG-TERM SETTLEMENT AND DEFORMATION OF HIGHWAY EMBANKMENTS ON SOFT FOUNDATIONS

**Tsutomu ISHIGAKI**

*NIPPO Corporation Research Institute, Tokyo, Japan  
ishigaki\_tsutomu@nippo-c.jp*

**Seiya YOKOTA**

*Nippon Expressway Research Institute, Tokyo, Japan*

**Hideki OHTA**

*Chuo University, Tokyo, Japan*

## ABSTRACT

Fundamental performance requirements of highway are to provide safety, serviceability and restorability. The performance required of highway embankments on soft foundations is that excessive settlement and deformation do not occur at the base which supports pavements and other road structures. In performance-based design and geotechnical asset management of highway, it may be necessary to accurately predict the long-term settlement and deformation of highway embankments. In this paper, a numerical assessment procedure of long-term settlement and deformation of highway embankments on soft foundations by the use of a soil / water coupled finite element analysis is proposed. The computer simulations to predict the long-term performance of embankments are carried out employing the soil / water coupled finite element program called DACSAR originally coded by Iizuka and Ohta (1987). The constitutive model mainly used in the analysis is an elastoviscoplastic model proposed by Sekiguchi and Ohta (1977). The author shows the applicability of numerical assessment procedure in engineering practice by carrying out a series of finite element analysis on two existing highway trial embankments in Hokkaido Expressway, Japan. The computed results are compared with the actual past performance of the embankments in full detail.

## 1. INTRODUCTION

The performance of embankments on soft foundations is dependent on many of primary factors practically uncontrollable by human management. Inevitable uncertainty generated by the nature of the work is the source of major difficulty in applying the performance-based design and geotechnical asset management to highway embankments on soft foundations. It appears to be essentially impossible to guarantee the required quality of embankments on soft foundations at a stage prior to actual construction works. However, the performance-based design and geotechnical asset management, in its nature, aims at designing more economical structures and minimizing life-cycle cost of maintenance while guaranteeing that the structures are fully qualified to a degree of required level. In order to overcome the difficulty arising from this contradiction, the author proposes a numerical assessment procedure to performance-based design and geotechnical asset management of embankments on soft foundations. Figure 1 summarizes the concept of the proposed procedure. Boxes A, B, C and D in Figure 1 form the conceptual flow of numerical assessment of performance-based design and geotechnical asset management that the author proposes for the use in designing and managing embankments on soft foundations. Basic process is as follows: [1]

- I. produce a prototype design (Box B) to fulfil the required performance of structures (Box A),
- II. produce, on the half-way of construction, revised designs by modifying the prototype design utilizing the information obtained from Class B predictions (defined by Lambe, 1973) [2] calibrated by the performance of the embankments monitored during prior construction (Box C),

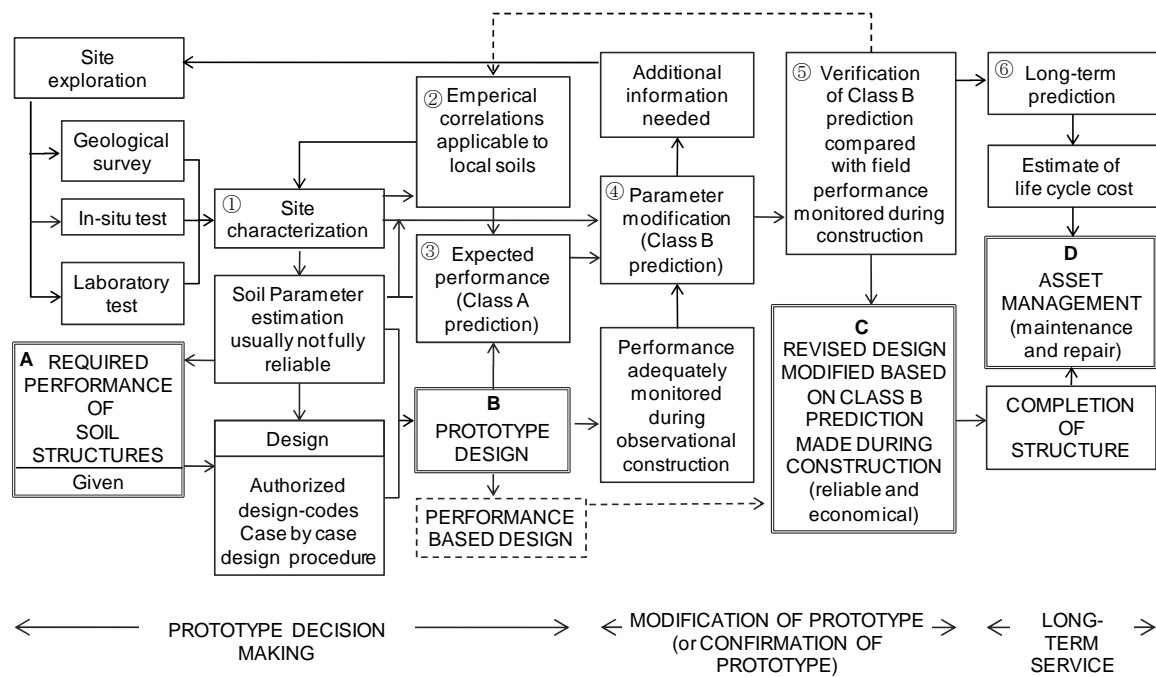


Figure 1 The concept of numerical assessment procedure of performance-based design and geotechnical asset management of highway embankment on soft ground [1]

- III. compare the prototype and revised designs and choose the most favourable design among them,
- IV. abandon the prototype design, in case that one of the revised designs is selected at stage (III), and continue constructing based on the revised design selected at stage (III) and
- V. utilize the long-term prediction obtained by extending the final Class B prediction in asset management of maintenance and repair works after opening to traffic (Box D).

In this paper, the authors' trial of the geotechnical performance-based design and geotechnical asset management is introduced following the boxes numbered from 1 through 6 indicated in Figure 1. Subsoil parameters (Box 1) estimated based on the soil testing and empirical correlations (Box 2) are used in the Class A prediction that produces the expected performance (Box 3) of the embankments. The expected performance of the embankments predicted by Class A prediction (Box 3) is compared with the actual performance of the embankments daily monitored in the progress of construction works. The comparison between expected and actually monitored performance of the embankments under construction can result in the subsoil parameter modification (Box 4) and revised Class B predictions being calibrated up to the latest stages of construction in the progress of works. Verification of logics and subsoil parameters used in the predictive analysis calibrated by the monitored performance (Box 5) strengthens the reliability of Class B predictions desirably at relatively early stage of construction. Placement of trial embankments prior to the full-scale embankments usefully works for such purpose in many cases. Calibration up to the latest stage of construction in the progress of works (Box 5) gives further reliability to the prediction. Thus calibrated Class B predictions can reliably work in producing several candidates of revised designs (Box C) elaborated based on verified Class B predictions. It is also possible at this stage of construction to estimate the life cycle cost of each candidate by predicting the long-term performance (Box 6) of each of the candidate revised designs with confidence. Selection of the best revised design (including the idea of going with the prototype design if it seems to be the best) should be made at this stage of construction when the revised design is still acceptable in the course of construction period. After the completion of the embankments, the long-term prediction should be calibrated from time to time and effectively used in the asset management (Box D).

Ishigaki (2009) propose the geotechnical performance-related indicators as mid-level indicator for use in geotechnical performance-based design and geotechnical asset management of highway embankment on soft foundations. Table1 show the examples of relationship between the geotechnical indicators and geotechnical performance-related indicators of highway embankment on soft foundation. The geotechnical indicators of highway embankments consist of settlement, vertical displacement and lateral displacement. These indicators are not only able to survey at site but to predict by the soil / water coupled finite element analysis. The geotechnical performance-related

Table 1 The relationship between the geotechnical indicators and geotechnical performance-related indicators of highway embankments on soft foundations [1]

Geotechnical indicator	Performance-related indicator	Performance requirement
settlement	- vertical alignment	- safety
	- cross slope	- serviceability
	- bridge approach settlement	- restorability
	- road width	
	- barrier height	- safety
lateral displacement of embankment toe / surrounding	- drainage	- restorability
	- stability	- safety
	- slope failure	- restorability
	- stability	- safety
	- slope failure	- restorability
vertical displacement of embankment toe / surrounding	- ground inclination	- safety
	- ground height	- restorability

indicators are mainly originated in road geometry. It can be considered that these indicators are related to the fundamental performance requirements of highway. The level of geotechnical performance-related indicators can be easily estimated from the value of geotechnical indicators. The author assumes the development of geotechnical performance-related indicators may be applicable and efficient for development of road performance indicators for use in performance-based design and geotechnical asset management. [1]

The recorded performance of two trial embankments for the Hokkaido Expressway constructed and intensely monitored during a period from 1977 through 1983 are used in this investigation. These two trial embankments are placed on soft peaty subsoil different from each other but empirical correlations (Box 2) should be applicable to both of these two sites. This makes it practically difficult to intentionally adjust the empirical correlations aiming at obtaining good agreement between predicted and monitored performance of two trial embankments.

## 2. ANALYZED SITE AND SUBSOIL PROPERTIES

The Hokkaido Expressway connecting Sapporo and Iwamizawa opened to traffic in 1983 after trial and error effort made during 5 years' construction period to ensure the stability of the embankment placed on highly compressive peat (about 700% of water content) underlain by alternative layers of soft clay and sand. The construction was carried out with very careful observation of settlement, lateral flow and pore water pressure generated by the placement of the fill. Stability of the fill was of primary importance and settlement was of secondary during the whole process of construction. Consequently long-term settlement of the road over the low peaty ground of 27km became a serious problem of the maintenance works in the past 25 years. Prior to the main construction works, trial embankments were placed in 1977 at Ebetsu and intensely monitored to collect the data of performance of the embankments and the foundations. In this investigation, performance records of the trial embankments NF1 and SD are used in comparison with the computed one. A trial embankment placed on the soft foundation without any countermeasures is named NF1 and that with sand-drains (0.4m in diameter, 10.1m long, 1.8m centre-to-centre pitch, triangular spacing) is named SD. Figure 2 shows the cross section and subsoil properties of Ebetsu trial embankment (SD). The fill bodies and counterweight berms of these trial embankments were placed directly on sand-mats (1.0m thick) overlying the peat layer. Drainage pipes (0.1m in diameter) were placed in the sand-mats from the centre to the toe of the fill body at every 4m interval along the longitudinal direction of the road. Very slow banking rate was adopted during the whole process of observational construction. The ground water levels at NF1 and SD are assumed, in the authors' analysis, to be GL -0.9m and GL -0.6m which are the annual averages of the ground water levels at the sites. [3] [4]

## 3. NUMERICAL MODELLING

The computer simulations to predict the performance of the trial embankments are carried out employing a soil / water coupled finite element program called DACSAR (Deformation Analysis

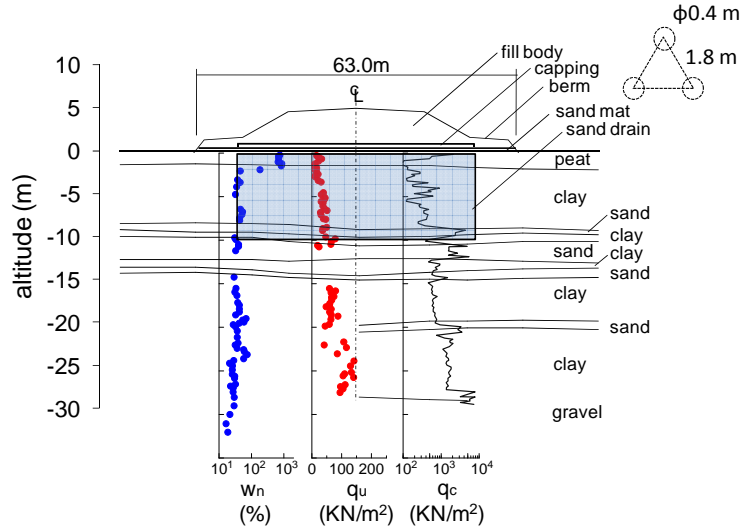


Figure 2 Cross section and subsoil properties of Ebetsu trial embankment (SD) [3]

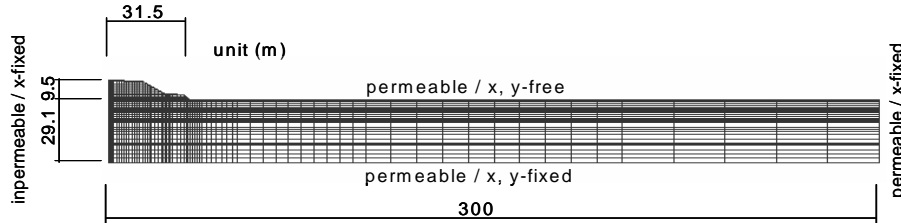


Figure 3 Finite element mesh of Ebetsu trial embankment (SD) [1]

Considering Stress Anisotropy and Reorientation) originally coded by Iizuka and Ohta (1987). [5] The constitutive model used in the analysis is an elasto-viscoplastic model proposed by Sekiguchi and Ohta (1977). The yield function of the elasto-plastic model is defined by:

$$f = MD \ln \frac{p'}{p'_0} + D\eta^* - \varepsilon_v^p = 0 \quad (1)$$

The flow function of elasto visco-plastic model is defined by:

$$F = \alpha \ln \left\{ 1 + \frac{t}{t_0} \exp \left( \frac{f}{\alpha} \right) \right\} - \varepsilon_v^p = 0 \quad (2)$$

where  $M$  = critical state parameter;  $D$  = coefficient of dilatancy proposed by Shibata (1963);  $p'$  = mean effective stress;  $p'_0$  = initial mean effective stress;  $\eta^*$  = generalized stress ratio proposed by Sekiguchi and Ohta (1977);  $\varepsilon_v^p$  = viscoplastic part of volumetric strain;  $\alpha$  = coefficient of secondary compression proposed by Sekiguchi and Ohta (1977);  $t$  = time;  $t_0$  = initial time. [6]

The model describes the inviscid behaviour of elasto-plastic soils as well as the time dependent on of the model is used to describe the mechanical behaviour of clays (Am: Alluvial (Holocene) silty clay) and inviscid (elasto-plastic) version of the model is used for peat (Ap: Alluvial (Holocene) peat). Fill bodies made of compacted soils, surface crust existing beneath SD embankment and sand layers (As: Alluvial (Holocene) sand) are described by using linearly elastic model.

The simulations are carried out at this moment 25 years after the completion of the road. They are "after event predictions" and therefore they are Class C predictions by the definition of Lambe (1973), but in a sense they are Class A predictions because no modification is made aiming at better agreement between computed and observed performances of the embankments during and after construction works. The author calls their first trial simulations of NF1 and SD embankments as Class A predictions. At the second stage, the author carries out the computer simulations by modifying the subsoil parameters pursuing better fitting. The authors consider the second series of simulations as Class B predictions which will further be utilized in long-term predictions.

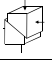
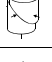
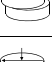
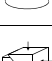
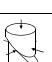

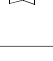
$\frac{c_u}{\sigma'_{v0}} = \frac{OCR^\lambda (1+2K_0) M \exp(-\Lambda)}{3\sqrt{3} (\cosh \beta - \sinh \beta \cos 2\theta)} \quad (9)$ $\frac{\tau}{\sigma'_{v0}} = \frac{OCR^\lambda (1+2K_0) M \exp(-\Lambda)}{3\sqrt{3} (\sqrt{\cosh^2 \beta - \cosh^2 \beta \cos^2 2\theta} - \sinh \beta \sin 2\theta)} \quad (10)$ $M = \frac{6 \sin \phi'}{3 - \sin \phi'} \quad \Lambda = 1 - C_s / C_c \quad \eta_0 = \frac{3(1-K_0)}{1+2K_0} \quad \beta = \frac{\sqrt{3}\eta_0\Lambda}{2M}$			
Type of test	Reduced equation for specified test on normally consolidated clay	Blue marine clay $I_p = 20$ $\phi' = 33$ $K_0 = 0.5$ Measured Predicted	
	$K_0$ -consolidated Plane strain Comp. $K_0PUC$ $\frac{c_u}{\sigma'_{v0}} = \frac{(1+2K_0) M \exp(-\Lambda)}{3\sqrt{3} (\cosh \beta - \sinh \beta)}$	0.34	0.347
	$K_0$ -consolidated Triaxial Comp. $K_0UC$ $\frac{c_u}{\sigma'_{v0}} = \frac{1+2K_0}{6} M \exp\left(\frac{\Lambda\eta_0}{M} - \Lambda\right)$	0.33	0.318
	Shear Box Test SBT $\frac{\tau}{\sigma'_{v0}} = \frac{(1+2K_0) M \exp(-\Lambda)}{3\sqrt{3}}$	-	0.239
	Direct Simple Shear DSS $\frac{\tau}{\sigma'_{v0}} = \frac{(1+2K_0) M \exp(-\Lambda)}{3\sqrt{3} \cosh \beta}$	0.20	0.224
	$K_0$ -consolidated Plane strain Ext. $K_0PUE$ $\frac{c_u}{\sigma'_{v0}} = \frac{(1+2K_0) M \exp(-\Lambda)}{3\sqrt{3} (\cosh \beta + \sinh \beta)}$	0.19	0.165
	$K_0$ -consolidated Triaxial Ext. $K_0UE$ $\frac{c_u}{\sigma'_{v0}} = \frac{1+2K_0}{6} M \exp\left(-\frac{\Lambda\eta_0}{M} - \Lambda\right)$	0.155	0.135
	Field Vane FV $\frac{\tau_u}{\sigma'_{v0}} = \frac{(1+2K_0) M \exp(-\Lambda)}{3\sqrt{3}}$ $\frac{\tau_v}{\sigma'_{v0}} = \frac{1+2K_0}{3\sqrt{3}} \sqrt{\left(\frac{Mp'}{\Lambda p'_0} \ln \frac{p'}{p'_0}\right)^2 - \left(1 - \frac{p'}{p'_0}\right)^2 \eta_0^2}$	0.19	0.182

Figure 4 Undrained strengths of Boston Blue Clay calculated based on the parameters reported by Ladd (1973) being compared with experimental undrained strengths obtained by Ladd (1973) [7]

Table 1 Empirical correlation for local peat and clays [8]

	clay (Am1)	clay(Am2-1)
$w_n(\%)$ - $Lig(\%)$	-	-
$w_n(\%)$ - $w_L(\%)$	$w_L = 0.978 w_n + 6.85$	$w_L = 0.826 w_n + 8.22$
$w_n(\%)$ - $e_i$	$e_i = 2.75 w_n / 100$	$e_i = 2.74 w_n / 100$
$w_L(\%)$ - $I_p(\%)$	$I_p = 0.77(w_L - 17)$	$I_p = 0.80(w_L - 17)$
$w_L(\%)$ - $C_c$	$C_c = 0.015(w_L - 20)$	$C_c = 0.016(w_L - 20)$
$C_c$ - $C_s$	$C_s = C_c / 10$	$C_s = C_c / 10$
$OCR$ - $\sigma'_{vi}$ (kN/m <sup>2</sup> )	$OCR = 4.02 - 0.594 \ln(\sigma'_{vi})$	$OCR = 3.14 - 0.406 \ln(\sigma'_{vi})$
	clay(Am2-2)	peat(Ap2-2)
$w_n(\%)$ - $Lig(\%)$	-	$w_n = 10 Lig$
$w_n(\%)$ - $w_L(\%)$	$w_L = 0.711 w_n + 15.45$	-
$w_n(\%)$ - $e_i$	$e_i = 2.65 w_n / 100$	$e_i = w_n / 100 \times 1 / (0.00237 Lig + 0.356)$
$w_L(\%)$ - $I_p(\%)$	$I_p = 0.75(w_L - 15)$	-
$w_L(\%)$ - $C_c$	$C_c = 0.014(w_L - 20)$	$C_c = 0.088 Lig$
$C_c$ - $C_s$	$C_s = C_c / 10$	$C_s = C_c / 10$
$OCR$ - $\sigma'_{vi}$ (kN/m <sup>2</sup> )	$OCR = 4.57 - 0.633 \ln(\sigma'_{vi})$	$OCR = 4.08 - 1.072 \ln(\sigma'_{vi})$

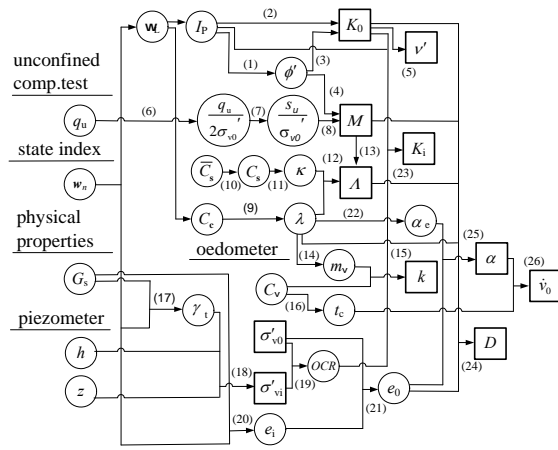
Finite element mesh of SD is shown in Figure 3. The cross sections are symmetric and finite element meshes are set to appropriately model the construction sequence as close to the actual sequence as possible. The analysis domain used in these simulations is about 10 times the width of embankment. The boundary drainage conditions are impermeable of the centre of embankment, and others are permeable. The embankment construction is modelled by adding elements to the mesh and the loading rate and the thickness of fill are assumed identical with those in the actual staged construction works. The buoyant force acting to the fill bodies submerged after settling are taken into account in the analysis.

#### 4. SUBSOIL PARAMETER DETERMINATION

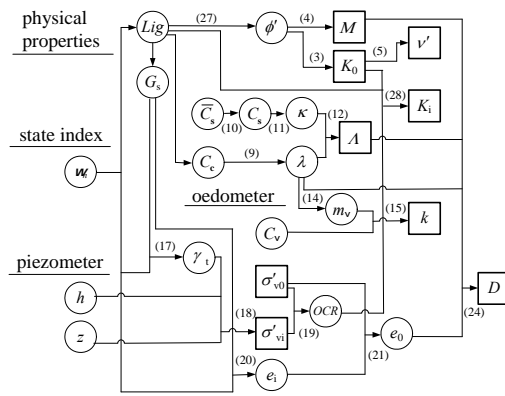
Since soils are generally much weaker than concrete and steel, major concern in designing soil structures is traditionally about strength of soil rather than deformability. For this reason, many of the soil testing methods used in geotechnical engineering practice are for estimating strengths of soils. Aiming at utilising traditional soil testing methods in specifying parameters needed in the model proposed by Sekiguchi and Ohta (1977) [5], equations for the undrained strengths to be obtained by different testing methods are theoretically derived by Ohta et al. (1985) [7] as summarised in Figure 4. Experimental values of undrained strengths of Boston Blue Clay measured by using different testing methods (Ladd, 1973) are in reasonably good agreement with those calculated from these theoretical equations using the material parameters reported by Ladd (1973) [2] as demonstrated in Figure 4 by Ohta et al. (1985). [7] Iizuka and Ohta (1987) [5] produced a flow chart for parameter determination employing these theoretical equations together with empirical equations obtained by many of past research workers. Through the experience of utilizing the flow chart proposed by Iizuka and Ohta (1987) [5] in simulating the performance of embankments on soft foundations, the authors found the usefulness of empirical correlations most likely applicable only to the local subsoil. These locally available relations are utilized by Ishigaki et al (2008) in producing Table 1. [8]

Determination of the input parameters of peat and clay layers is made, in this investigation, by employing the charts shown in Figure 5 after modifying Iizuka and Ohta 's flow chart. [8]

Young's modulus of the crust immediately beneath the trial embankment SD is specified by using correlation between the cone bearing capacity and deformation parameters after Sanglerat (1972). Poisson's ratio of the crust is estimated from  $K_0$ -value of peat layer. Young's moduli and permeability coefficients of sand layers are estimated after Lunne and Chistophersen (1983) and Creager et al. (1945) while Poisson's ratio is assumed as 1/3. Young's moduli of compacted fill



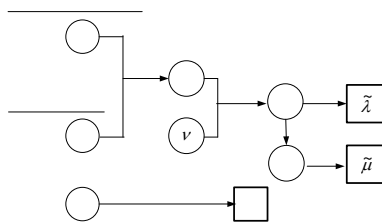
(a) clay



(b) peat

- (1)  $\sin \phi' = 0.81 - 0.233 \log I_p$  Kenny (1959)
- (2)  $K_0 = 0.44 + 0.42 \times 10^{-2} I_p$  Massarsch (1979)
- (3)  $K_0 = 1 - \sin \phi'$  Jaky (1944)
- (4)  $M = 6 \sin \phi' / (3 - \sin \phi')$
- (5)  $v' = K_0 / (1 + K_0)$
- (6)  $(q_u / 2 \sigma'_{v0})_{NC} = 1 / (OCR)^{A/4} (q_u / 2 \sigma'_{v0})_{OC}$  Ohta (1988)
- (7)  $(S_u / \sigma'_{v0})_{CK0UC} = \mu (q_u / 2 \sigma'_{v0})_{NC}$  Ohta (1988)
- (8)  $M$  determined using  $(S_u / 2 \sigma'_{v0})_{CK0UC}$  Ohta (1988)
- (9)  $\lambda = 0.434 C_c$
- (10)  $\bar{C}_s / C_s = 1 - \log \beta / \log(OCR)$   
 $\beta = (1 + 2 K_i) / (1 + 2 K_0)$
- (11)  $\kappa = 0.434 C_s$
- (12)  $A = 1 - \kappa / \lambda$
- (13)  $A = M / 1.75$  Karube (1975)
- (14)  $m_v = 3 \lambda / ((1 + e_0)(1 + 2 K_0) \sigma'_{v0})$
- (15)  $k = m_v C_v \gamma_w$
- (16)  $t_c = H^2 T_v(90\%) / C_v$  Sekiguchi (1977)
- (17)  $\gamma_t = G_s \gamma_w (1 + w_n) / (1 + G_s w_n)$
- (18)  $\sigma'_{vi} = \gamma_t z - p_w$
- (19)  $OCR = \sigma'_{v0} / \sigma'_{vi}$
- (20)  $e_i = G_s w_n$
- (21)  $e_0 = e_i - \lambda (1 - A) \ln(OCR)$   
 $OCR = OCR (1 + 2 K_0) / (1 + 2 K_i)$
- (22)  $\alpha_e / \lambda = 0.05 \pm 0.02$  (for clay) Mesri &  
 $\alpha_e / \lambda = 0.07 \pm 0.02$  (for peat) Godlewshi (1977)
- (23)  $K_i = K_0 (OCR)^m$  Alpan (1967)  
 $m = 0.54 \exp(-I_p / 122)$  (for clay)
- (24)  $D = \lambda A / (M(1 + e_0))$  Ohta (1971)
- (25)  $\alpha = \alpha_e / (1 + e_0)$  Sekiguchi (1977)
- (26)  $\dot{v}_0 = \alpha / t_c$  Sekiguchi (1977)
- (27)  $\phi' = 0.19 Lig + 32$  (for peat) Hayashi (2005)
- (28)  $K_i = K_0 (OCR)^m$  Hayashi (2006)  
 $m = 0.005 Lig + 0.45$  (for peat)

Figure 5 Parameter determination chart of peat and clays [8]



- (29)  $E_{oed} = M = \alpha q_c$  Sanglerat (1972)  
(for peat and organic clay)  
50 < w\_n < 100% 1.5 < α < 4  
100 < w\_n < 200% 1.0 < α < 1.5  
200 < w\_n 0.4 < α < 1.0  
(for NC sand)  
q\_c < 10 Mpa α = 4  
10 Mpa < q\_c < 50 Mpa M = 2 q\_c + 20  
50 Mpa < q\_c α = 120  
(for OC sand)  
q\_c < 50 Mpa α = 5  
50 Mpa < q\_c α = 250
- (30)  $M = E_{oed} = (1 - \nu) E / (1 - 2 \nu) (1 + \nu)$
- (31)  $E = 2 G (1 + \nu)$
- (32)  $\tilde{\lambda} = \nu E / (1 + \nu) (1 - 2 \nu)$
- (33)  $\tilde{\mu} = G$
- (34)  $K$  determined using D20 Creager (1945)

Figure 6 Parameter determination chart of sand and crust [1]

material, capping layer and sand mat are assumed by reference to the authors' past experiences and permeability coefficients of these materials are estimated after Creager, Justin and Hinds (1945). Poisson's ratio of these elastic materials is assumed as 1/3. Parameter determination chart of sand and crust is shown in Figure 6.

Figures 7 and 8 (a) through (f) indicate the raw data of subsoil layers in NF1 and SD. [3]

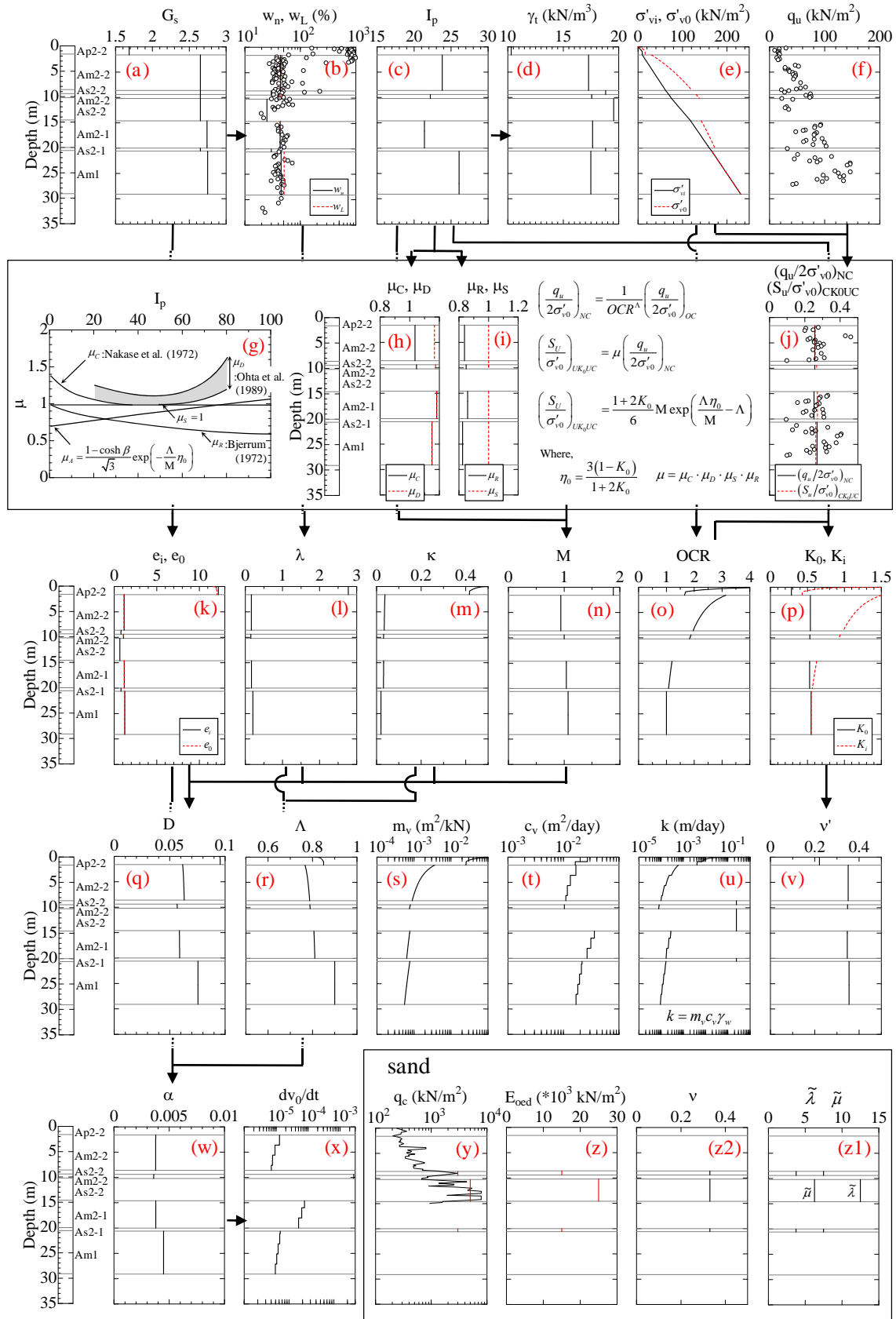


Figure 7 Flow of specifying subsoil parameters beneath Trial embankment NF1 [1]

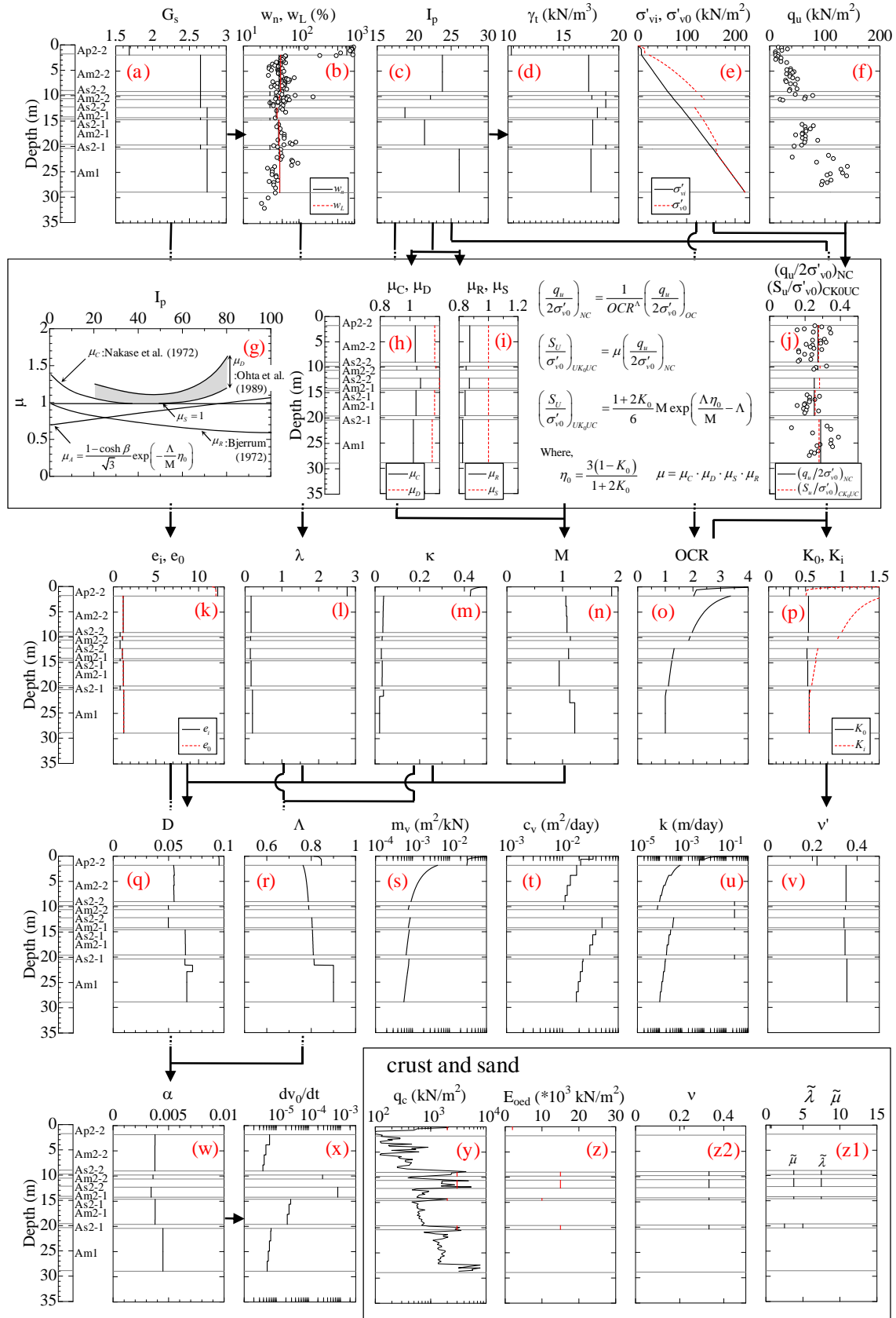


Figure 8 Flow of specifying subsoil parameters beneath Trial embankment SD [1]



The data of site investigation are only natural water content ratio (b) and unconfined compressive strength (f), and other data are calculated by utilizing Table 1, Figure 5 and Figure 6. Figures 7 and Figures 8 (k) through (z2) show the results of thus specified subsoil parameters of peat and clays needed in the constitutive model proposed by Sekiguchi and Ohta (1977). [5] Permeability  $k$  of peat and clay decreases with the reduction of void ratio  $e$  resulting from the progress of consolidation process. In many cases,  $e$  plotted against  $\ln k$  makes a straight line in the similar fashion to  $e$ - $\ln p'$  relation the gradient of which is compression index  $\lambda$ . In this investigation, the gradient  $\lambda_k$  of  $e$ - $\ln k$  line is assumed to be equal to compression index  $\lambda$  after the investigation by Ohta et al. (1984).

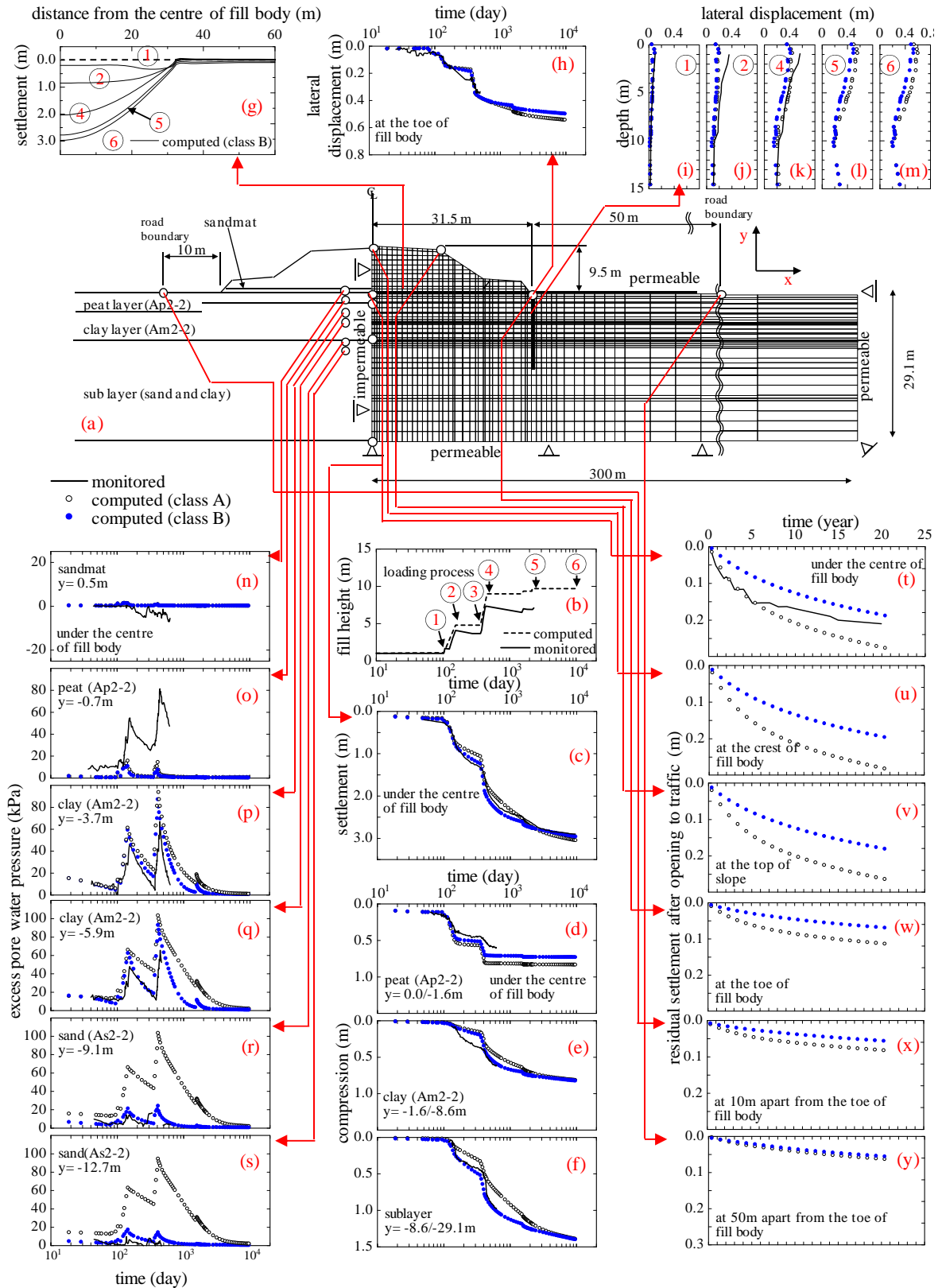
Three dimensional effect of sand drains installed in the soft foundation beneath the trial embankment SD is two-dimensionally modelled by using the apparent coefficient of permeability converted in a method that the apparent consolidation coefficient is obtained so that the 50% consolidation time calculated by the theory of Yoshikuni (1979) becomes identical with that calculated by Terzaghi's one dimensional consolidation theory. Furthermore, the influence of well resistance is also taken into consideration. The multiplying factor of a coefficient of permeability is calculated assuming the consolidation time using the theory of Barron, and the consolidation time using the theory of Terzaghi to be equal. This multiplying factor gives a coefficient that converts permeability from 3D to 2D. In case of the trial embankment SD, this factor are assumed as resulting in a conversion factor of 10 that means the permeability of peat and clay obtained from the laboratory tests are multiplied by a factor of 10 for the sand drained foundation of the trial embankment SD. Three dimensional effect of drainage pipes installed in the sand-mat beneath the trial embankment NF1 and SD is two-dimensionally modelled by using the apparent coefficient of permeability converted by use of the theory of Sera (1992). [1]

## 5. NUMERICAL ASSESSMENT OF TRIAL EMBANKMENTS

The actual performance of the trial embankments NF1 and SD monitored during and after construction being compared with the performance predicted by Class A and Class B predictions are shown.

Figures 9 and Figures 10 (a) show the overall configuration and location of monitoring instruments. [3] Figures 9 and Figures 10 (b) show the loading process of the fill plotted against time. [3] Both loading processes of NF1 and SD were almost the same. Computed loading process shown by dotted line indicates the fill thickness placed on the ground while the monitored fill height shown by solid line indicates the height of the fill. The difference between these two lines shows the amount of settlement. It is very important to take construction process into consideration to analysis in order to obtain reliable analysis results. Figures 9 and Figures 10 (c) show the settlement of the fill under the centre of fill body. Both of the settlement curves of computed results are relatively good agreement with the monitored one. However, it is seen that the Class A prediction shown by open circles are in poorer agreement with the monitored long-term settlement if compared with the Class B prediction shown by solid circles. Figures 9 and Figures 10 (d) through (f) show the compression of the subsoil layers under the centre of fill body. In comparisons, the predictive accuracy of the lower layer (clay of Am2-2 and sub layer) of class B analysis improves. It is considered that predictive accuracy improved by correction of the parameter according a coefficient of permeability of sand layers to class B analysis.

Figures 9 and Figures 10 (g) show the computed settlement bowls by class B prediction. Figures 9 and Figures 10 (h) show the monitored lateral displacement at the toe of the fill compared with Class A and Class B predictions. Figures 9 and Figures 10 (i) through (m) show the profiles of the lateral displacement beneath the toe of the embankment. The deformation modes of computed results are relatively good agreement with the monitored one. When considering the stability of a filling during construction and the influence on the circumference during operation, these predictions of lateral deformation may give important decision-making materials for designers and constructors. Figures 9 and Figures 10 (n) through (s) show the pore water pressure generated in the foundation. The performance of Class B prediction is in much better agreement with the monitored pore water pressure. It should be noted here that Class A prediction is made by employing the subsoil parameters obtained in the previous section, but Class B prediction is made in this case by modifying only the permeability of the sandy layers without modifying any other parameters. Figure 11 shows the permeability of sandy layers originally estimated for Class A prediction and the permeability modified for Class B prediction. As demonstrated in Figures 9 and 10, the predicted pore water pressure drastically changes before and after modification of permeability of sandy layers and consequently Class B prediction gives much better agreement with the monitored values. Figures 9 and 10 (n) through (s) evidence reasonably trustful predictability of Class B prediction made by the use of the integrated technique of modelling, parameter determination and computer simulation introduced in this paper. This implies that Class B predictions represented by period after opening to traffic.



Figures 9 Monitored and predicted performances (Class A and Class B predictions) of Trial embankment NF1 [1]

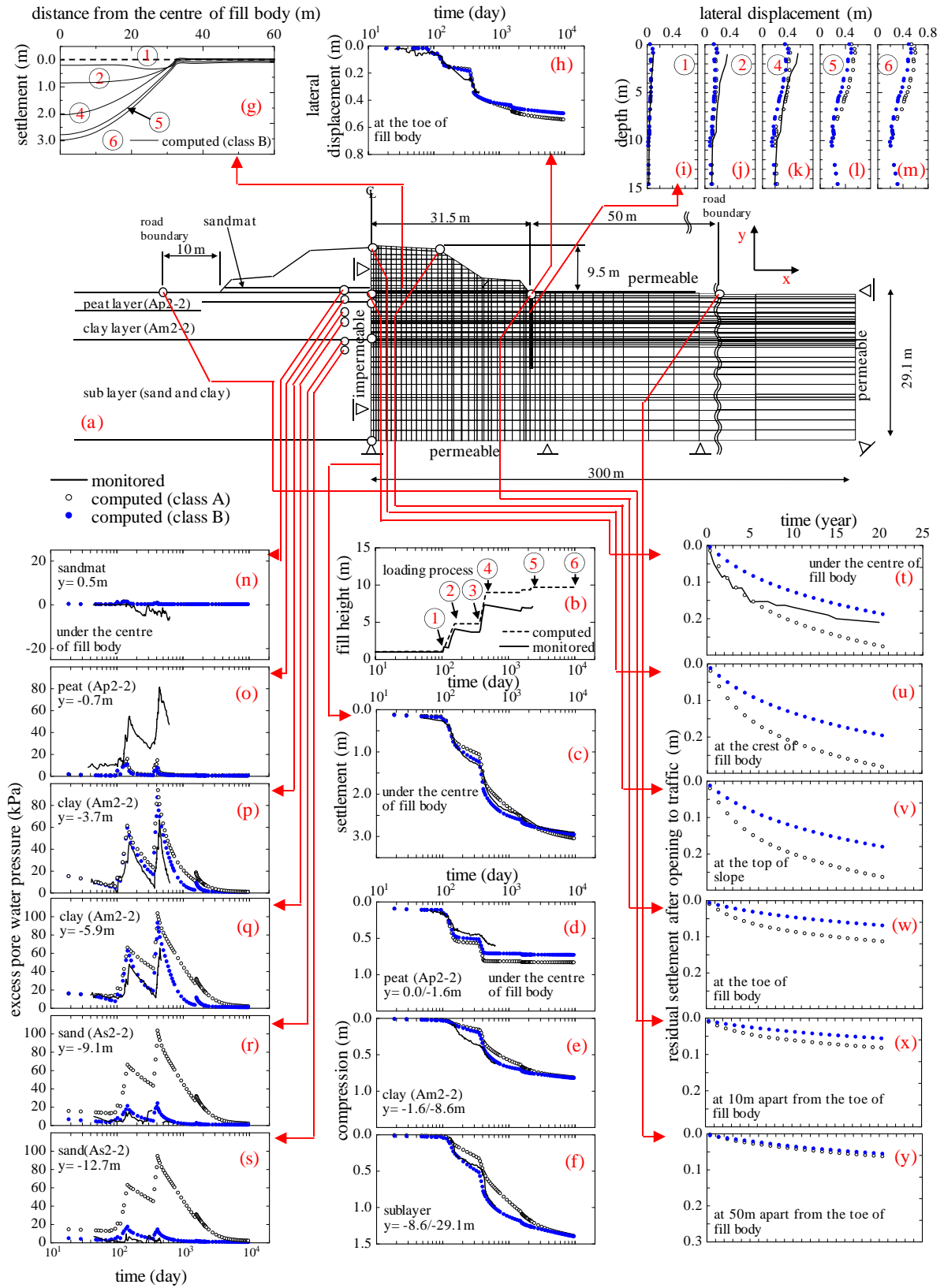


Figure 10 Monitored and predicted performances (Class A and Class B predictions) of Trial embankment SD [1]

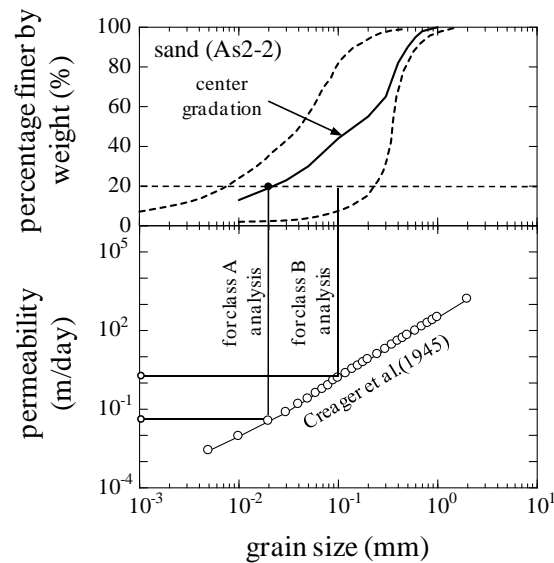


Figure 11 Permeability of sandy layers originally estimated for Class A prediction and the permeability modified for Class B prediction [1]

## 6. CONCLUDING REMARKS

Actual performances of highway embankments placed on soft foundations depend on many of primary factors practically uncontrollable by human management. Inevitable uncertainty generated by the nature of the work makes it unrealistic expectation to guarantee the required quality of embankments at a stage prior to actual construction works. This is because of relatively poor predictability of the current techniques of Class A prediction which is the prediction before the event starts to take place. In order to fill the gap arising from this contradiction, a numerical assessment procedure of performance-based design and geotechnical asset management of highway embankments on soft foundations is proposed in this investigation. It is obvious that reasonably trustful Class B predictions made on the half-way of construction work should be carried out by effectively employing the proposed procedure in the engineering practice. Trials of making Class B predictions of the possible performances of two trial embankments placed on very soft foundations evidenced in this paper that the current technique of a soil/water coupled finite element analysis is reliable enough to be used in the performance-based design and geotechnical asset management of highway embankments on soft foundations.

## REFERENCES

1. T. Ishigaki. Geotechnical Management of Highway Embankment on Soft Clay. Doctor Thesis. Tokyo Institute of Technology. 2009
2. TW. Lambe. Prediction in Soil Engineering. Geotechnique 23. pp 149-202. 1973
3. Japan Highway Public Corporation. Report of Central Hokkaido Highway, Ebetsu Trial Embankment. 1979 (in Japanese)
4. Japan Highway Public Corporation. Report of Central Hokkaido Highway (Sapporo- Iwamizawa), Survey of long-term settlement of soft foundation. 2005 (in Japanese)
5. H.Sekiguchi. and H.Ohta. Induced anisotropy and time dependency in clays, Constitutive Equation of Soils, Proc. 9th International Conference on Soil Mechanics and Foundation Engineering, Specialty Session 9, 305-315. 1977
6. A. Iizuka and H.Ohta. A determination procedure of input parameters in elasto-viscoplastic finite element analysis. Soils & Foundation. Vol.27. No.3. pp71-87.1987
7. H.Ohta. A.Nishihara and Y.Morita. Undrained stability of  $K_0$ -consolidated clays. Proc.11th ICSMFE. Vol.2. pp613-616.1985
8. T.Ishigaki. S.Omoto. A.Iizuka. T.Takeyama. and H.Ohta. Numerical modelling for life cycle planning of highway embankment on soft foundation. Proc, of 1st International Conference on Transportation Geotechnics. Advances in Transportation Geotechnics, CRC Press. Taylors & Francis Group. pp389-395. 2008